Introduction to GPS Radio Occultation

Stig Syndergaard

COSMIC Project Office
University Corporation for Atmospheric Research

FORMOSAT-3/COSMIC Science Summer Camp, Taipei, May 30–June 3, 2005

Topics of lecture

The basics

- The GPS radio occultation principle
- GPS observations (what is the signal?)
- Derived products (what comes out of it?)

Inversion of GPS radio occultation data

- From signal to products (next slide)

Advanced topics

- Atmospheric multipath propagation
- Super refraction

Topics of lecture (continued)

Inversion of GPS radio occultation data

- Excess phase $\longrightarrow$ excess Doppler
- Excess Doppler $\longrightarrow$ bending angle
  - Correction for Earth's oblateness
  - Ionospheric correction
  - Statistical optimization
- Bending angle $\longrightarrow$ refractivity
  - The Abel transform (the core of the data inversion)
- Refractivity $\longrightarrow$ pressure, temperature & humidity

Ionospheric data

- Phase differential $\longrightarrow$ total electron content (TEC)
- Total electron content $\longrightarrow$ electron density

The GPS radio occultation principle

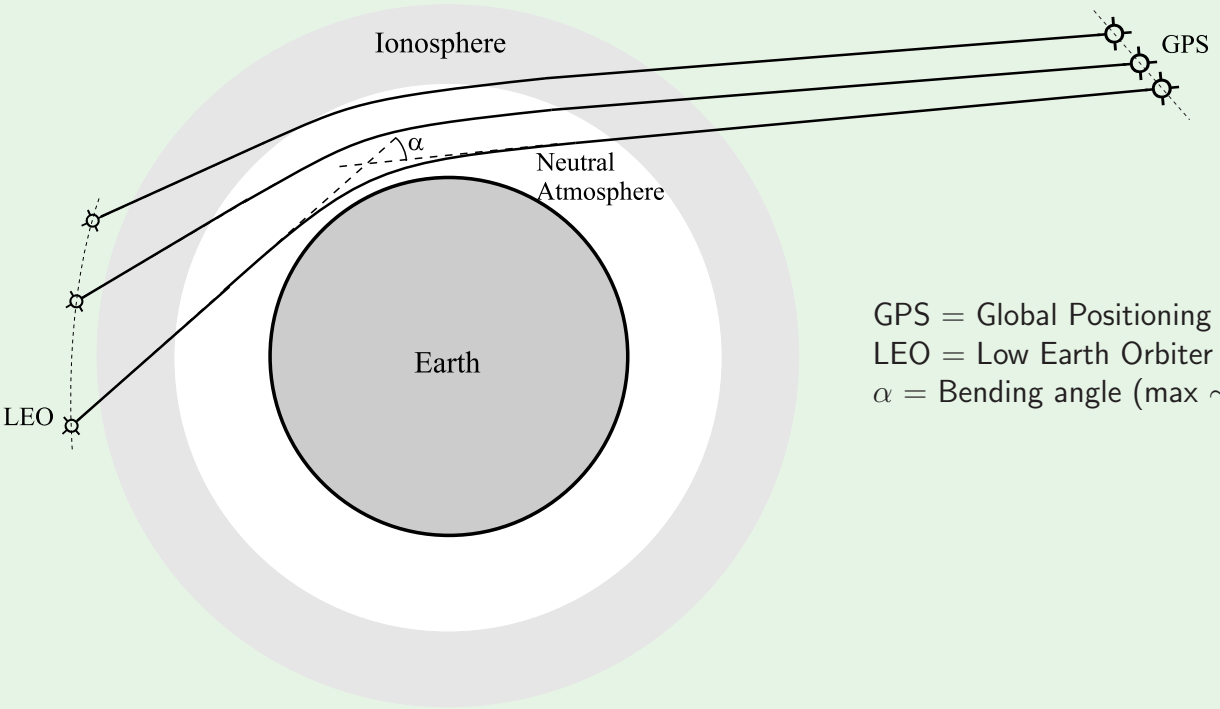

GPS = Global Positioning System
LEO = Low Earth Orbiter
α = Bending angle (max $\sim 2°$)

Signal frequencies: $f_1 = 1.57542\,\text{GHz}$ & $f_2 = 1.22760\,\text{GHz}$

Refractive index of medium: $n \approx 1 + 77.6\frac{p}{T} + 3.73\times 10^5 \frac{e}{T^2} + 40.3\frac{N_\text{e}}{f^2}$

Basic GPS occultation observations

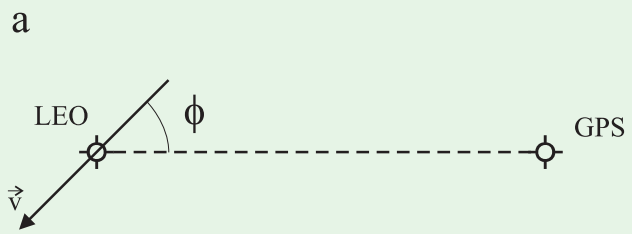

a) The Doppler depends on Φ and $\vec{v}$

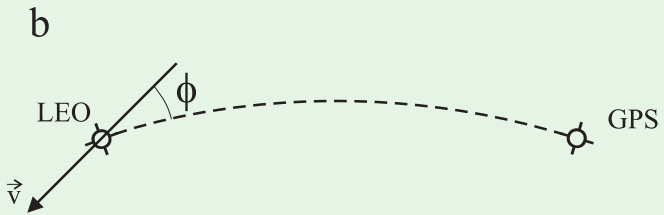

b) With bending, the Doppler is different than expected from velocities only

Basic measurement is a phase path (meters): $L = \int_{\mathrm{GPS}}^{\mathrm{LEO}} n \, \mathrm{d}s$

Excess phase (path) is defined as: $\Delta L = L - |\vec{r}_{\mathrm{LEO}} - \vec{r}_{\mathrm{GPS}}|$

We are interested in the phase change: excess Doppler $= \mathrm{d}\Delta L/\mathrm{d}t$

The bending effect

Curved signal path through the atmosphere

- The signal path is curved according to Snell's law because of changes in the index of refraction along the path
- In a spherically symmetric medium, Snell's law is replaced by Bouger's law:

$$nr \sin \psi = a = \text{constant}$$

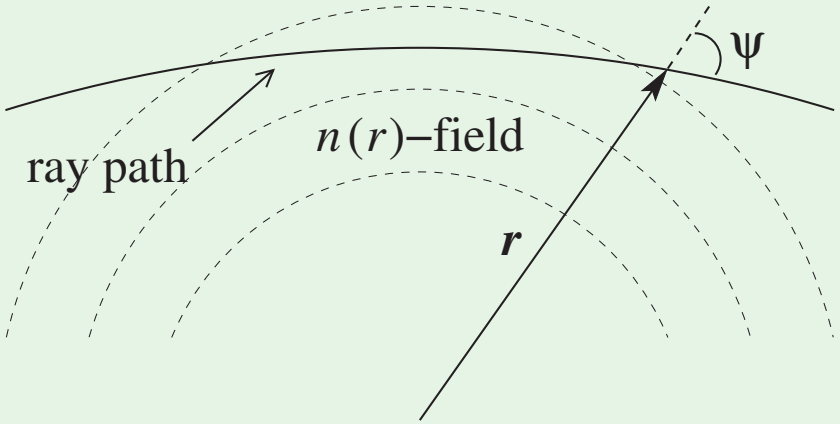

The bending effect

Bouger's law leads to (e.g., Fjeldbo et al. 1971):

$$\alpha(a) = -2a \int_{r_0}^{\infty} \frac{\mathrm{d} \ln n/\mathrm{d}r}{\sqrt{n^2 r^2 - a^2}} \mathrm{d}r$$

where bending toward the Earth is counted positive and r_0 is the radius at the tangent point: $n(r_0)r_0 = a$

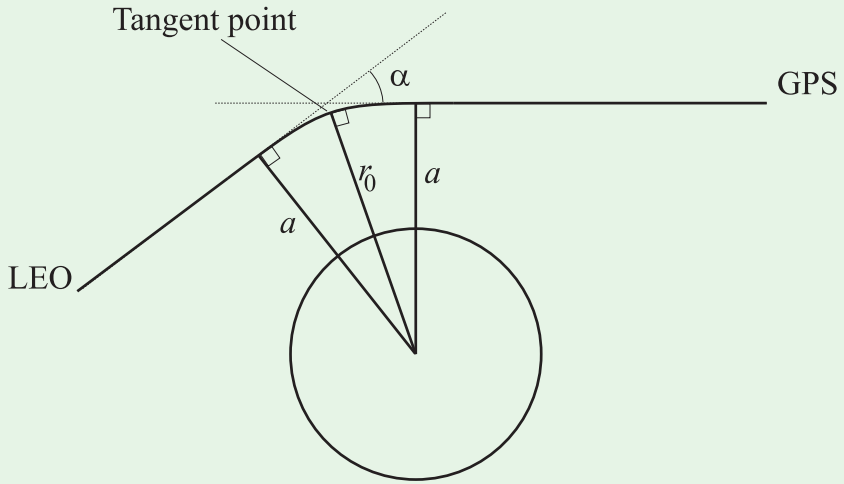

Derived data products

Basic assumption: local spherical symmetry

- Bending angle as a function of impact parameter, a (ray asymptote)
  - Numerical weather prediction & Climate research
- Refractivity (defined as $N = (n-1) \times 10^6$) as a function of altitude
  - Numerical weather prediction & Climate research
- Temperature, pressure (geopotential height), and humidity profiles
  - Atmospheric & Climate research

Ionospheric data

- Total electron content between GPS and LEO
  - Input to space weather models
- Electron density as a function of altitude
  - Ionospheric research

Data product characteristics

Accuracy of derived refractivity

- Mean accuracy less than 0.5% between 2 and 25 km
- Standard deviation less than 1% between 5 and 25 km
- In the troposphere: Accuracy limited by horizontal gradients
- Above ∼30 km: accuracy limited by thermal and ionospheric noise
- Below ∼2 km: tracking errors may dominate

Vertical resolution

- ∼100 m in lower troposphere, increasing to ∼1.5 km in stratosphere

Ionospheric data

- Accuracy of electron density profiles limited by horizontal gradients
- Vertical resolution determined by sampling rate (∼2 km for 1 Hz data)

Data processing chain

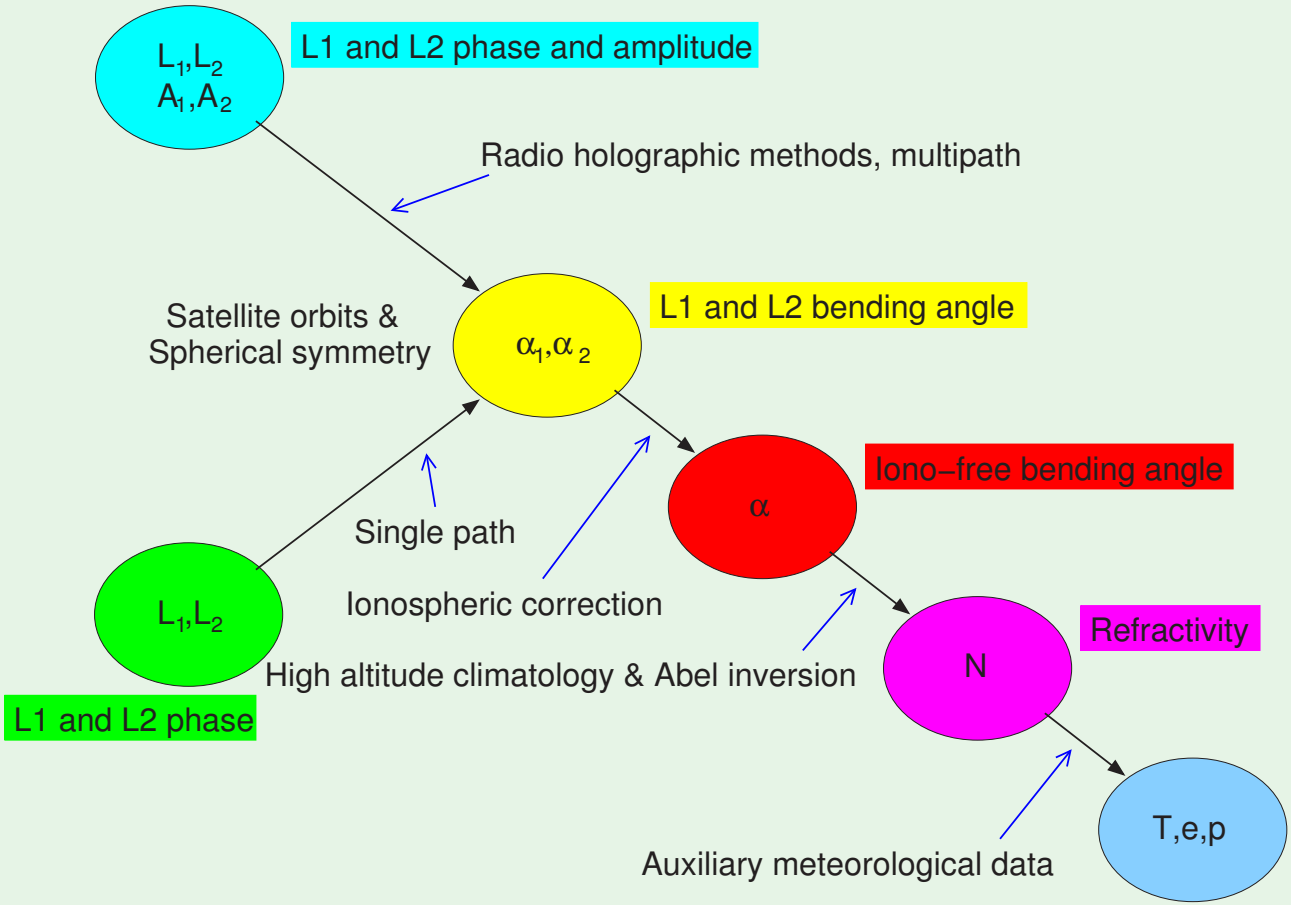

Excess phase — what does it look like?

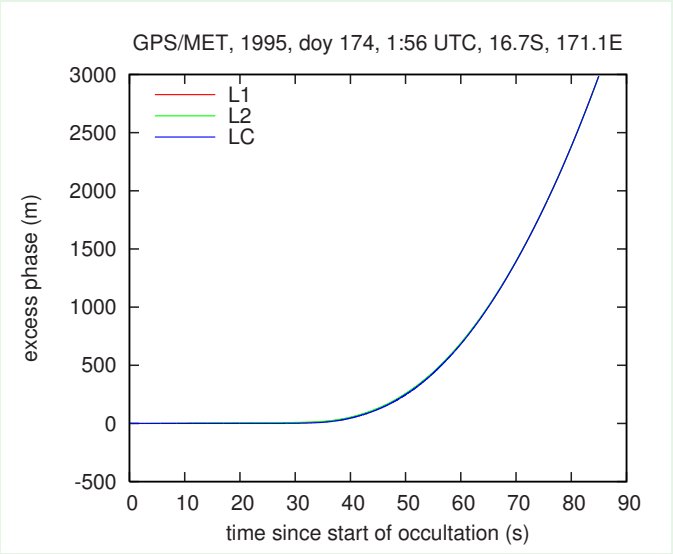

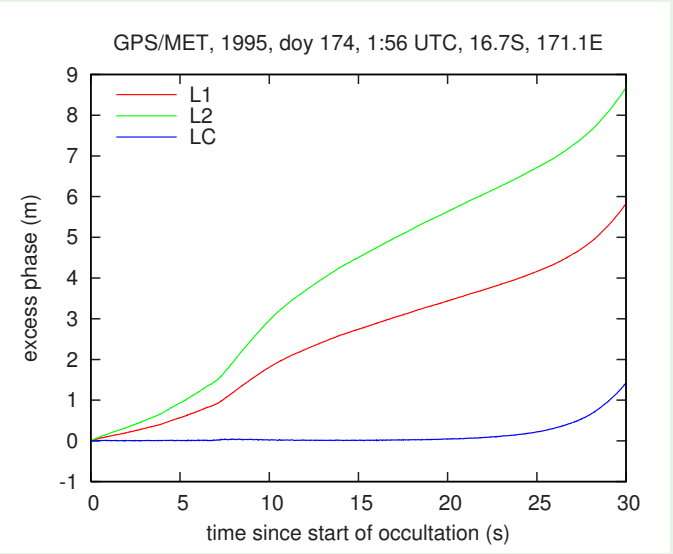

- An occultation typically lasts about 1 minute (sometimes more)
- The excess phase can become as large as a few km near the surface

$$\Delta L_{\mathrm{C}}(t) = \frac{f_1^2 \Delta L_1(t) - f_2^2 \Delta L_2(t)}{f_1^2 - f_2^2} = L_{\mathrm{C}}(t) - |\vec{r}_{\mathrm{GPS}} - \vec{r}_{\mathrm{LEO}}|$$

Excess phase — what does it look like?

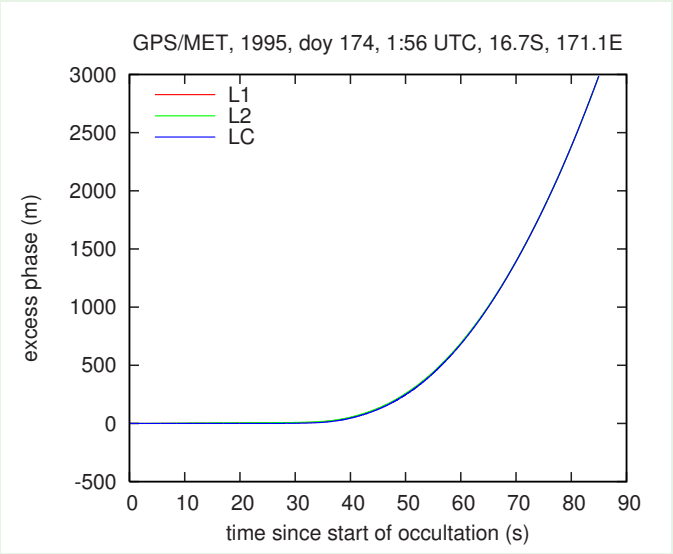

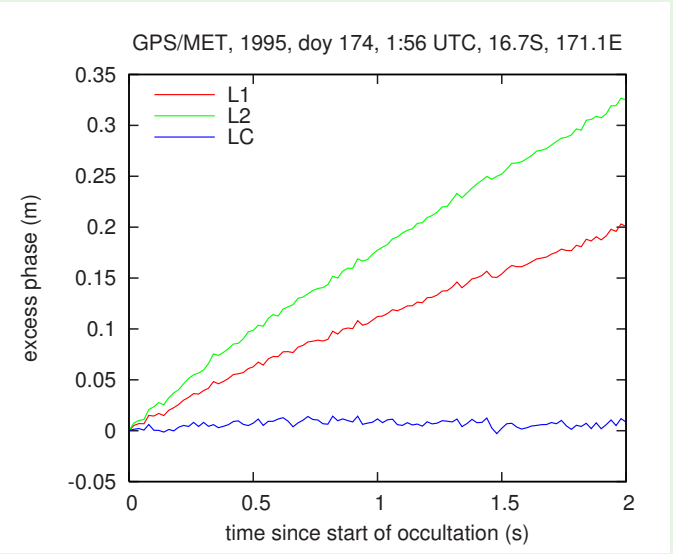

- An occultation typically lasts about 1 minute (sometimes more)
- The excess phase can become as large as a few km near the surface

$$\Delta L_{\mathrm{C}}(t) = \frac{f_1^2 \Delta L_1(t) - f_2^2 \Delta L_2(t)}{f_1^2 - f_2^2} = L_{\mathrm{C}}(t) - |\vec{r}_{\mathrm{GPS}} - \vec{r}_{\mathrm{LEO}}|$$

Excess Doppler — what does it look like?

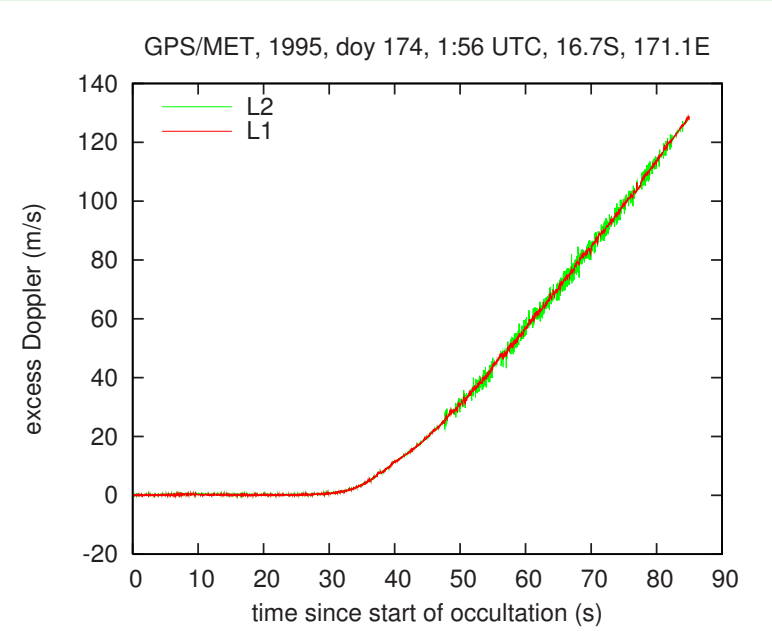

$$\Delta D = \frac{\mathrm{d}\Delta L}{\mathrm{d}t}$$

Usually smoothing (low pass filtering) is applied to the excess phase before the excess Doppler is derived (not in this plot, though)

- L2 signal is affected by Anti-Spoofing (encryption of the P-code) which leads to a low signal-to-noise ratio, in turn leading to tracking errors in the lower troposphere (L2 not used in lower troposphere)

Excess Doppler $\longrightarrow$ bending angle

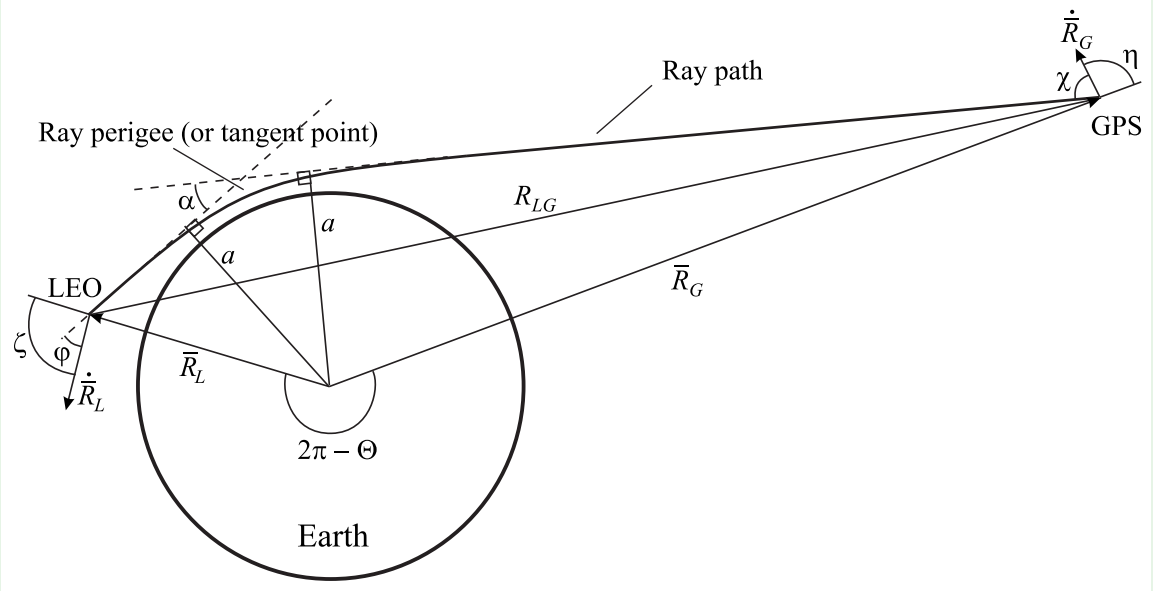

- Having satellite positions & velocities (from precise orbit determination)
- Having the excess Doppler (from observations)
- Assuming spherical symmetry then determines the impact parameter, a, and subsequently the bending angle, α

Excess Doppler $\longrightarrow$ bending angle

$$\Delta D(t) \longrightarrow \boxed{\begin{gathered} \Delta D + \dot{R}_{\mathrm{LG}} - \left(|\dot{\bar{R}}_{\mathrm{L}}| \cos\varphi(a) - |\dot{\bar{R}}_{\mathrm{G}}| \cos\chi(a) \right) = 0 \\ \varphi(a) = \zeta - \arcsin\left(\frac{a}{|\bar{R}_{\mathrm{L}}|} \right) \\ \chi(a) = (\pi - \eta) - \arcsin\left(\frac{a}{|\bar{R}_{\mathrm{G}}|} \right) \\ \alpha = \Theta - \arccos\left(\frac{a}{|\bar{R}_{\mathrm{L}}|} \right) - \arccos\left(\frac{a}{|\bar{R}_{\mathrm{G}}|} \right) \end{gathered}} \longrightarrow \alpha(a)$$

(e.g., Melbourne et al. 1994)

- Bending angle derived from Doppler is used in the stratosphere and perhaps upper troposphere, but not in the lower troposphere
- In the moist lower troposphere, multipath propagation may be present, and more advanced methods has to be used to derive the bending angle (more about this later)

Correction for Earth's oblateness

- The Earth is slightly oblate (elliptical) such that the center of curvature does not match the center of the Earth in general
- The center of curvature varies with position on the Earth and the orientation of the occultation plane

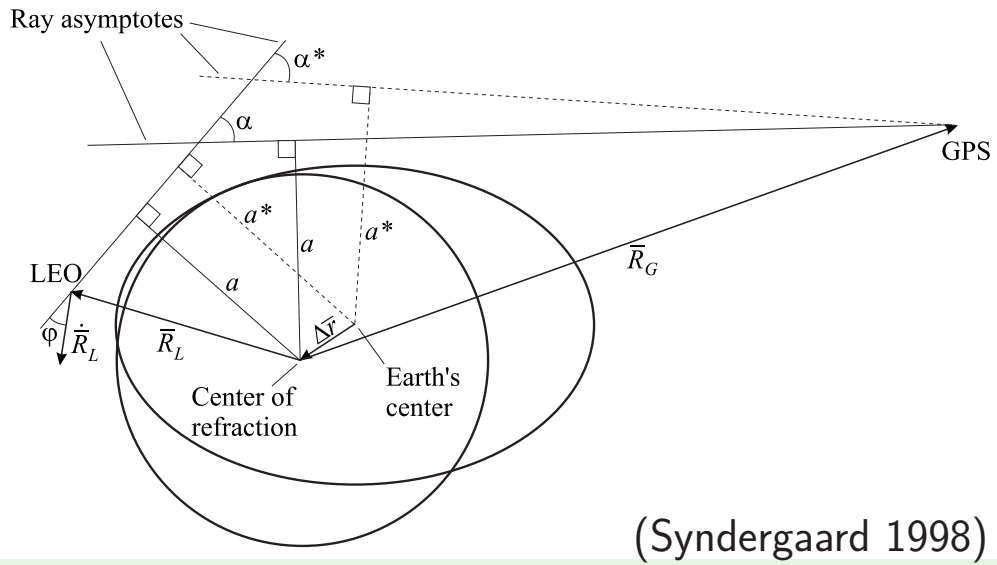

(Syndergaard 1998)

- α and a are estimated with respect to the center of a circle in the occultation plane that best fits the ellipsoid near the tangent point

Ionospheric correction of bending angles

Consider approximate equations for the L1 and L2 bending angles:

$$\alpha_i(a) \approx -2a \int_a^\infty \frac{\mathrm{d}}{\mathrm{d}x}\left(10^{-6} N_\mathrm{n} - \frac{40.3}{f_i^2} N_\mathrm{e}\right) \frac{\mathrm{d}x}{\sqrt{x^2 - a^2}}$$

The ionosphere-free bending angle is formed from the derived bending angles at the same impact parameter (Vorob'ev and Krasil'nikova 1994):

$$\alpha(a) = \frac{f_1^2 \alpha_1(a) - f_2^2 \alpha_2(a)}{f_1^2 - f_2^2} \approx -2a \int_a^\infty 10^{-6} \frac{(\mathrm{d}N_\mathrm{n}/\mathrm{d}x)\mathrm{d}x}{\sqrt{x^2 - a^2}}$$

- Ionospheric correction of phases assumes that the L1 and L2 signal paths are identical (but the ionosphere is dispersive)
- Ionospheric correction of bending angles at equal impact parameters ensures that the involved L1 and L2 signal paths are close to each other near the tangent point (and that is an advantage)

Statistical optimization

- Formally, we need bending angles to infinite altitudes in order to derive the refractivity (of course we don't have that)
- Bending angles are contaminated with thermal noise and residual noise from ionospheric turbulence
- Fractionally the noise increases exponentially with altitude rendering the bending angle useless at some altitude and above

"Optimal" estimation of bending angle:

$$\tilde{\alpha}(a) = \alpha_{\mathrm{model}}(a) + \frac{\sigma^2_{\mathrm{model}}}{\sigma^2_{\mathrm{model}} + \sigma^2_{\mathrm{obs}}}[\alpha(a) - \alpha_{\mathrm{model}}(a)]$$

α_{model} is estimated from a climatological model
σ_{obs} may be evaluated from the data above the stratosphere
σ_{model} is usually set to a fixed number (20%)

Bending angle — what does it look like?

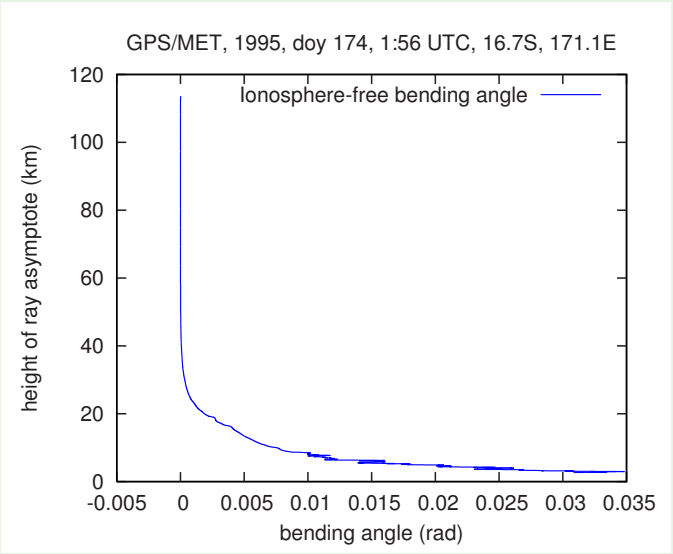

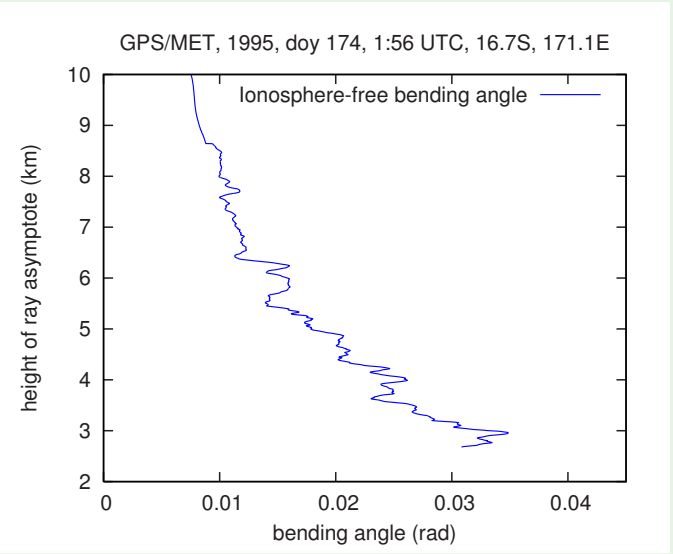

- Bending is significant only below $\sim$25 km (but still important above)
- The bending angle may be as large as 0.035 rad (2°) near the surface
- In the lower troposphere, moisture variations causes large fluctuations in the bending angle (multipath propagation, which I will get to shortly)

Bending angle — what does it look like?

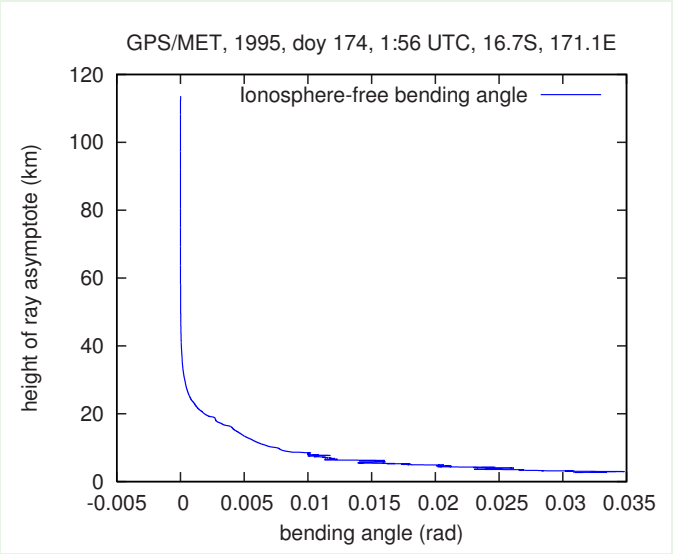

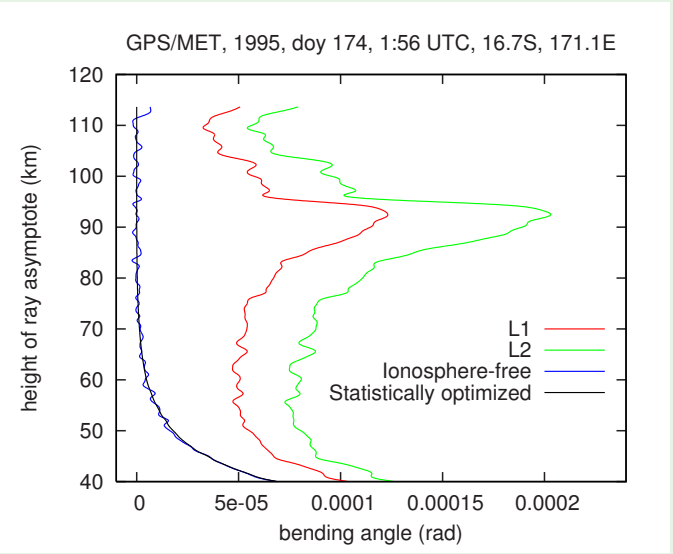

- Bending is appreciable only below ∼25 km (but still important above)
- The bending angle may be as large as 0.035 rad (2°) near the surface
- In the lower troposphere, moisture variations causes large fluctuations in the bending angle (multipath propagation, which I will get to shortly)

Bending angle $\longrightarrow$ refractivity

$$\alpha(a)$$
$$\downarrow$$

Abel integral transform (e.g., Fjeldbo 1971)

$$\alpha(a) = -2a \int_{r_0}^{\infty} \frac{\mathrm{d} \ln n / \mathrm{d}r}{\sqrt{n^2 r^2 - a^2}} \mathrm{d}r \quad \Longleftrightarrow \quad n(r_0) = \exp\left(\frac{1}{\pi} \int_a^{\infty} \frac{\alpha(x)}{\sqrt{x^2 - a^2}} dx \right)$$

$$r_0 = \frac{a}{n(r_0)} \quad , \quad N(r_0) = 10^6 \times (n(r_0) - 1)$$

$$\downarrow$$
$$N(r)$$

- The Abel integral transform relies on the assumption of spherical symmetry
- It provides a simple and unique solution to an otherwise underdetermined inverse problem
- In practice the integration is performed to some high altitude where the bending angle can be neglected (above 100 km)

Refractivity — what does it look like?

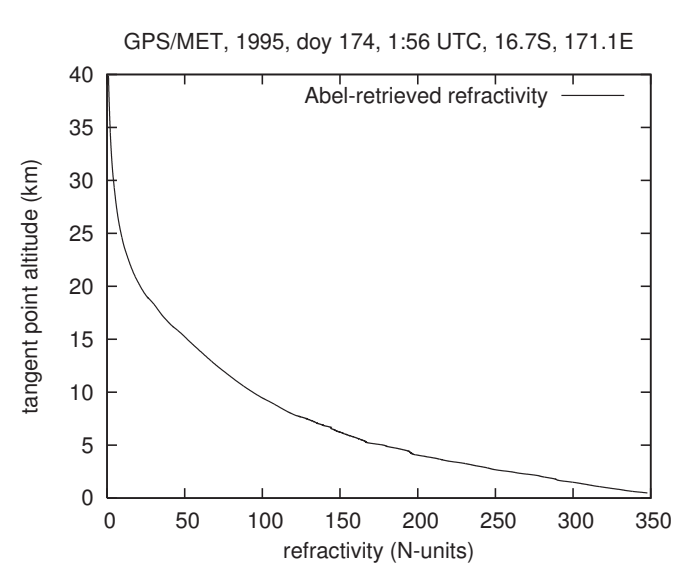

- The *inverse* Abel integral (going from bending angle to refractivity) acts as a low pass filter, somewhat similar to the operator of a half integration
- Possibly the product that will be assimilated at most NWP centers in the near future

Refractivity $\longrightarrow$ pressure & temperature

Refractivity equation:

$$N \approx 77.6\frac{p}{T} + 3.73 \times 10^5 \frac{e}{T^2}$$

- Two terms: a dry (or hydrostatic) term and a wet term
- The wet term can be neglected at temperatures less than $\sim$240 K (i.e., at few kilometers above the surface at high latitudes and above $\sim$10 km at tropical latitudes)

Neglecting the wet term:

$$N(r) \longrightarrow \boxed{\begin{array}{c} N = 77.6\frac{p}{T} \quad , \quad p = \rho R_\mathrm{d} T \\ \\ \frac{\mathrm{d}p}{\mathrm{d}z} = -\rho g \quad , \quad z = r - r_\mathrm{curv} \end{array}} \longrightarrow p(z), T(z)$$

Temperature — what does it look like?

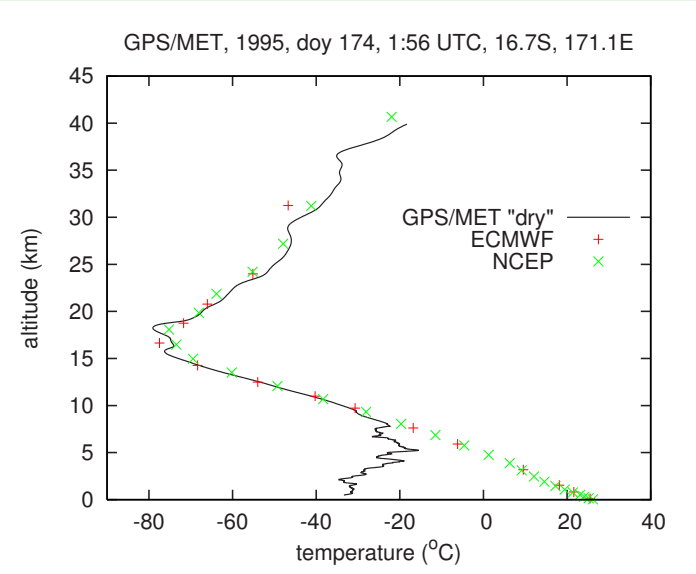

- The temperature derived by neglecting water vapor is called the "dry temperature"
- The dry temperature significantly underestimates the actual temperature in the lower moist troposphere

Deriving water vapor pressure

Two common ways of deriving water vapor:

1. include additional information about the actual temperature profile and solve directly for water vapor (iterative procedure)
2. One-dimensional variational technique optimally combining the refractivity profile with information from an NWP model

Method number 1:

$$N(z), T_{\text{apriori}}(z)$$

$$\downarrow$$

$$e = T^2 \frac{N - 77.6(p_\text{d} + e)/T}{3.73 \times 10^5} \quad , \quad \frac{\text{d}(p_\text{d} + e)}{\text{d}z} = -(\rho_\text{d} + \rho_\text{w})g$$

$$p_\text{d} = \rho_\text{d} R_\text{d} T \quad , \quad e = \rho_\text{w} R_\text{w} T$$

$$\downarrow$$

$$e(z), p_\text{d}(z)$$

Deriving water vapor pressure

Method number 2 (variational retrieval):

- Include information about errors in a priori temperature, pressure and water vapor, as well as errors in the observed refractivity

$$N(z), T_{\text{apriori}}(z), p_{\text{apriori}}(z), e_{\text{apriori}}(z)$$

$$\downarrow$$

Minimizing the following cost function:

$$J(\mathbf{x}) = (\mathbf{x} - \mathbf{x}_\text{b})^\text{T}\mathbf{B}^{-1}(\mathbf{x} - \mathbf{x}_\text{b}) + (\mathbf{N}_\text{obs} - \mathbf{N}(\mathbf{x}))^\text{T}\mathbf{R}^{-1}(\mathbf{N}_\text{obs} - \mathbf{N}(\mathbf{x}))$$

$\mathbf{x}$ is the state vector to be solved for

$\mathbf{x}_\text{b}$ is the a priori state vector

$\mathbf{N}(\mathbf{x})$ is the refractivity equation

$\mathbf{B}$ is the a priori error covariance matrix

$\mathbf{R}$ is the observation + representativeness error covariance matrix

$$\downarrow$$

$$T(z), p(z), e(z)$$

Water vapor — what does it look like?

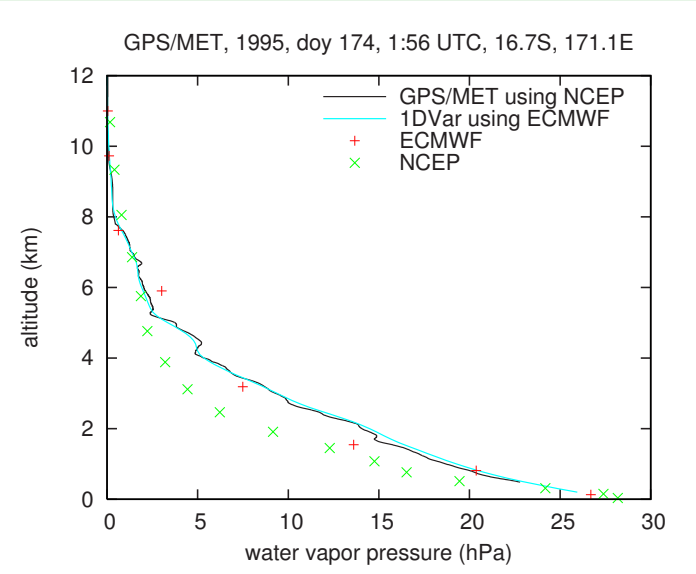

- The two methods result in almost the same water vapor profiles
- 1DVar retrieval is presumably the most accurate, since it includes most information, but the very high vertical resolution is lost

A few words about ionospheric data

- Bending throughout (most of) the ionosphere can be ignored

Definition of total electron content: $\mathrm{TEC} = 10^{-16} \int_{\mathrm{GPS}}^{\mathrm{LEO}} N_{\mathrm{e}} \mathrm{d}s$

Our observations: $L_i = \int_{\mathrm{GPS}}^{\mathrm{LEO}} (10^{-6} N_{\mathrm{n}} - \frac{40.3}{f_i^2} N_{\mathrm{e}}) \mathrm{d}s$

$L_1(t), L_2(t)$

$\downarrow$

$$\mathrm{TEC} = \frac{L_1 - L_2}{40.3 \times 10^{16}} \frac{f_1^2 f_2^2}{f_1^2 - f_2^2}$$

$\downarrow$

$\mathrm{TEC}(r)$

$\mathrm{TEC}(r)$

$\downarrow$

$$N_{\mathrm{e}}(r_0) = \frac{10^{16}}{\pi} \int_{r_0}^{r_{\mathrm{LEO}}} \frac{\mathrm{dTEC}/\mathrm{d}r}{\sqrt{r^2 - r_0^2}} \mathrm{d}r$$

$\downarrow$

$N_{\mathrm{e}}(r)$

- $\mathrm{dTEC}/\mathrm{d}r$ is proportional to the bending angle

Ionospheric profiles — what do they look like?

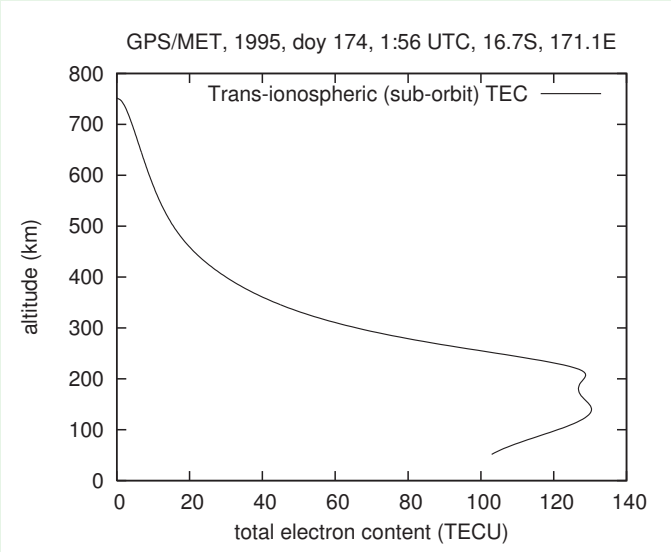

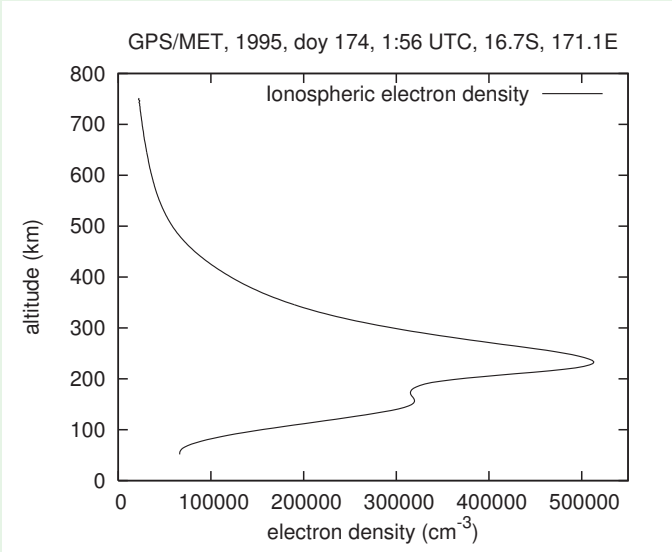

- TEC calibrated with positive elevation angle data (Schreiner et al. 1999)
- Retrieval of N_{e} is based on the assumption of spherical symmetry
- The spherical symmetry assumption may result in large under-estimation or over-estimation of electron density in the lower part of profiles

ADVANCED TOPICS

- **Atmospheric multipath propagation**
- **Super refraction**

Multipath propagation

Atmospheric multipath propagation refers to the situation where there are more than one signal path (Fermat's principle) between the transmitter (GPS) and the receiver (LEO)

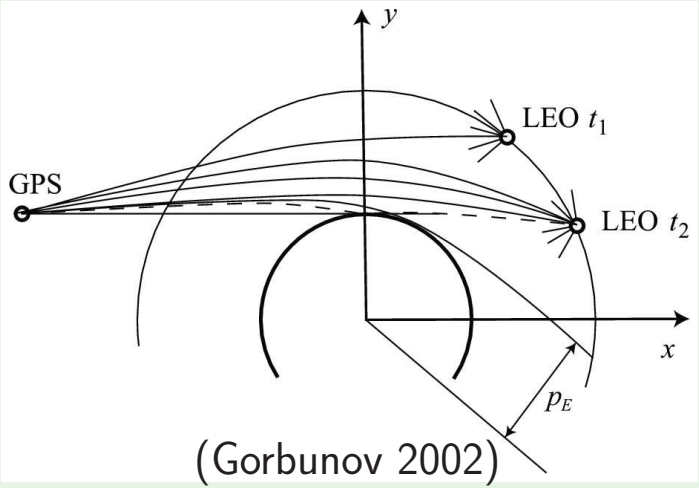

(Gorbunov 2002)

- Multipath propagation is a result of sharp vertical refractivity gradients varying rapidly with height (due to the water vapor term)
- Multipath propagation can be expected in the lower troposphere in regions with large amounts of water vapor

Multipath propagation

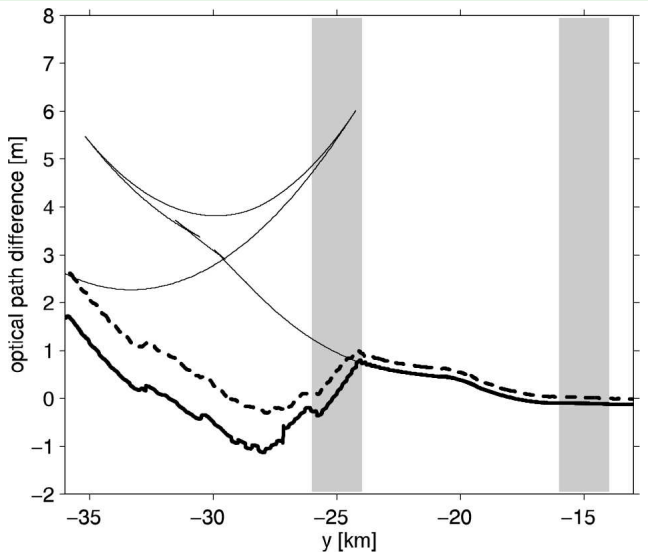

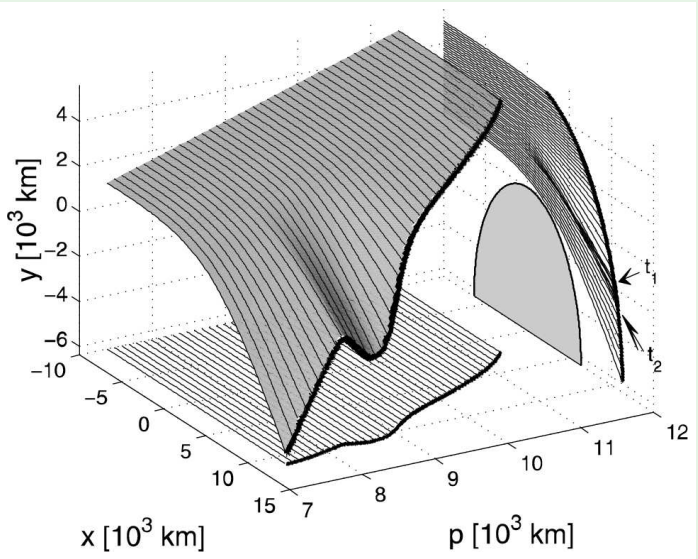

(Beyerle et al. 2003)

- Multipath propagation results in interference in the phase measurements
- We need to disentangle the multipath because the Abel transform is based on the assumption of single ray propagation
- Radio-holographic methods basically transform the measured signal from geometrical space to impact parameter space where multipath is absent

Phase & amplitude $\longrightarrow$ bending angle

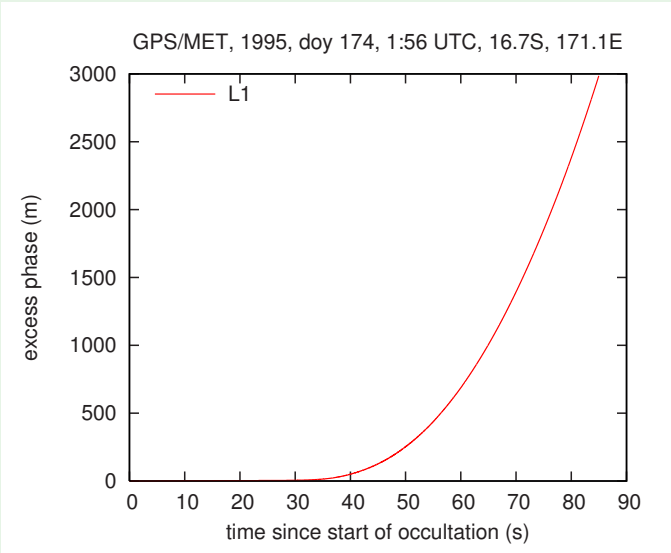

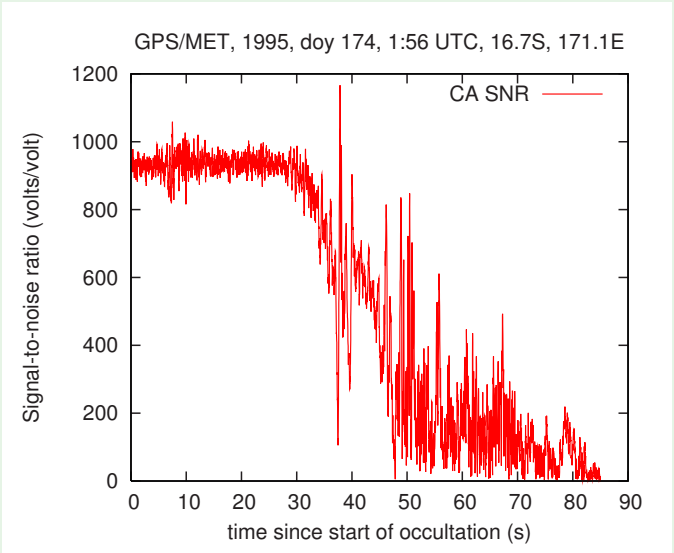

- Both phase and amplitude is used in radio-holographic methods

$A\exp(ik\Delta L_1) \rightarrow$ [redacted] $\rightarrow \alpha_1(a)$

Phase & amplitude $\longrightarrow$ bending angle

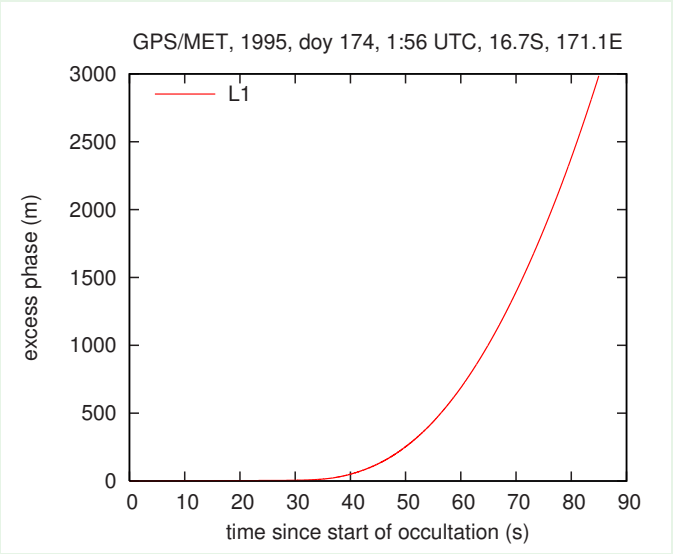

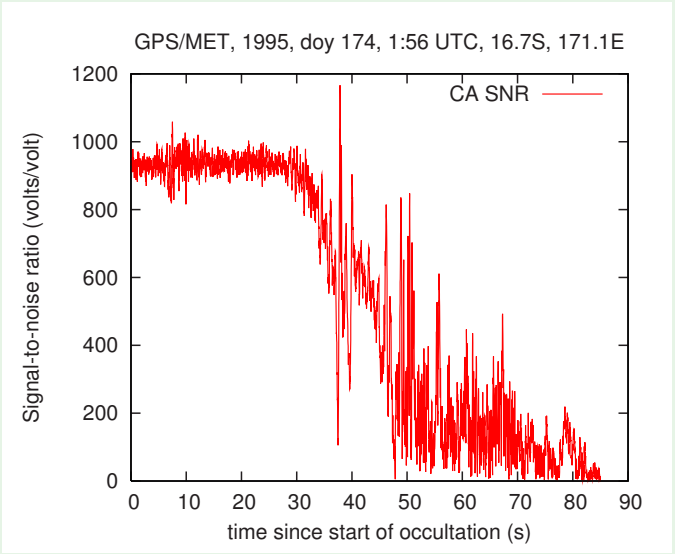

- Both phase and amplitude is used in radio-holographic methods

$A\exp(ik\Delta L_1) \longrightarrow$

Back propagation (Gorbunov 1998)
Sliding spectrum (Sokolovskiy 2001)
Canonical transform (Gorbunov 2002)
Full spectrum inversion (Jensen et al. 2003)
etc.

$\longrightarrow \alpha_1(a)$

Bending angle — different methods

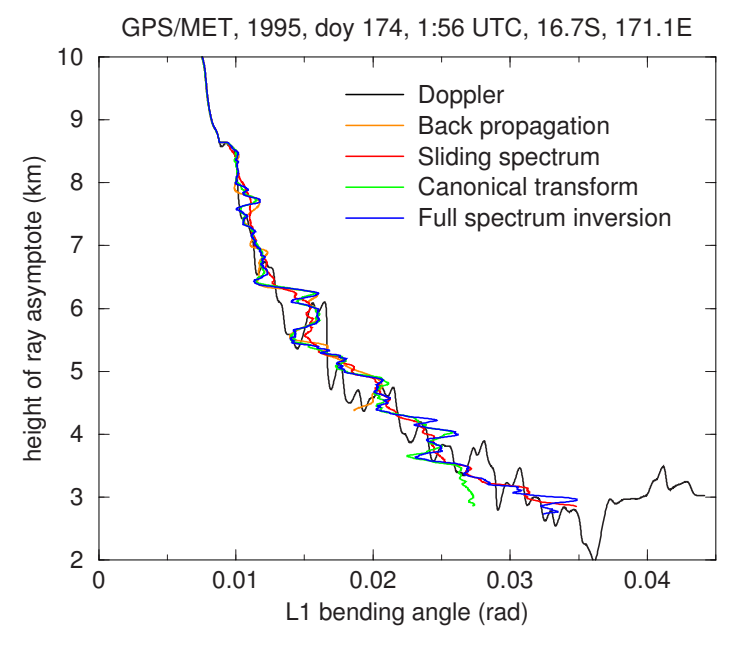

- Deriving the bending angle in the lower troposphere using Doppler may result in multivalued bending angle as a function of impact parameter
- Different radio-holographic methods give almost the same answer, but Full Spectrum Inversion (FSI) is at present the most commonly used

Super refraction

Super refraction refers to the situation when the bending becomes so large (locally) that the curvature of a ray exceeds the curvature of the atmosphere

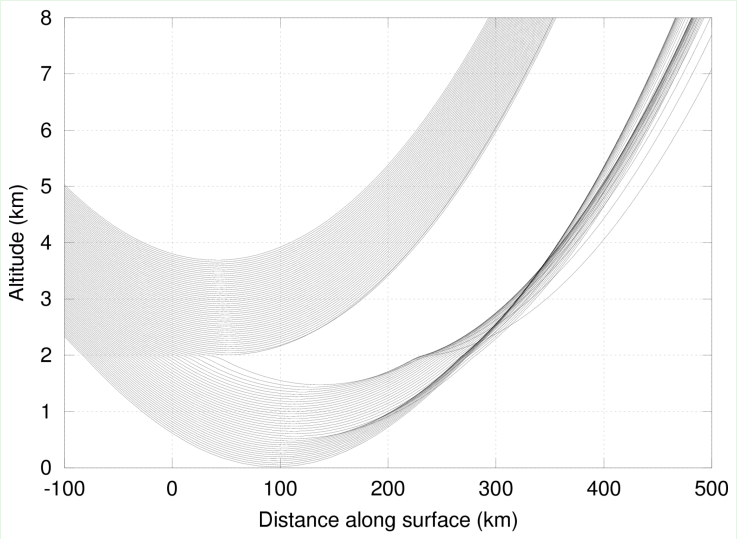

Critical refraction point:

$$\mathrm{d}N/\mathrm{d}r \approx -157\,\text{N-units/km}$$

Super refraction:

$$\mathrm{d}N/\mathrm{d}r < -157\,\text{N-units/km}$$

Ducting layer in this figure:

Between 1.5 and 2 km

- No ray path connecting satellites can exist with a tangent point altitude within a layer just below the critical refraction point
- A signal launched horizontally within this layer will be trapped or ducted

Super refraction

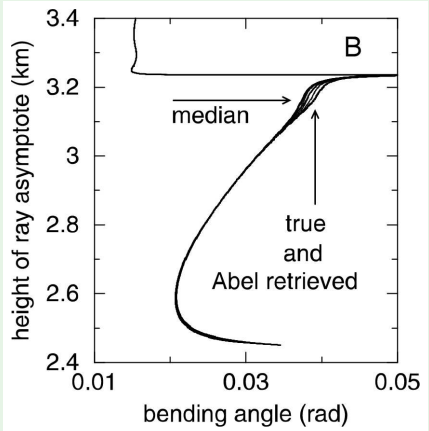

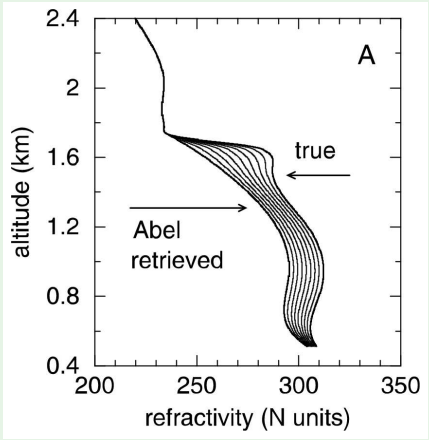

(Sokolovskiy 2003)

- Super refraction may happen near the top of the moist marine boundary layer
- Bending angle theoretically goes to infinity at the critical refraction point
- Applying the Abel transform gives a negative refractivity bias below the critical refraction point
- There is in fact an infinite number of different refractivity profiles corresponding to identical bending angle profiles
- Super refraction is largely an unsolved problem for GPS radio occultation
  - Super refraction is not easy to detect in the data (poses a problem for NWP)
  - We do not really know how to handle it properly even if we could detect it

References and suggested reading

Beyerle, G., M. E. Gurbunov, and C. O. Ao, 2003: Simulation studies of GPS radio occultation measurements. *Radio Sci.*, **38**, 1084, doi:10.1029/2002RS002800.

Fjeldbo, G., A. J. Kliore, and V. R. Eshleman, 1971: The neutral atmosphere of Venus as studied with the Mariner V radio occultation experiments. *Astron. J.*, **76**, 123–140.

Gorbunov, M. E., 2002: Canonical transform method for processing radio occultation data in the lower troposphere. *Radio Sci.*, **37**, 1076, doi:10.1029/2000RS002592.

Gorbunov, M. E., 2002: Ionospheric correction and statistical optimization of radio occultation data. *Radio Sci.*, **37**, 1084, doi:10.1029/2000RS002370.

Gorbunov, M. E., 2002: Radio-holographic analysis of microlab-1 radio occultation data in the lower troposphere. *J. Geophys. Res.*, **107**, doi:10.1029/2000JD000889.

Gorbunov, M. E. and A. S. Gurvich, 1998: Algorithms of inversion of Microlab-1 satellite data including effects of multipath propagation. *Int. J. Remote Sens.*, **19**, 2283–2300.

Healy, S. B., 2001: Smoothing radio occultation bending angles above 40 km. *Ann. Geophys.*, **19**, 459–468.

Healy, S. B. and J. R. Eyre, 2000: Retrieving temperature, water vapour and surface pressure information from refractive-index profiles derived by radio occultation: A simulation study. *Quart. J. Roy. Meteorol. Soc.*, **126**, 1661–1683.

Jensen, A. S., M. S. Lohmann, H.-H. Benzon, and A. S. Nielsen, 2003: Full spectrum inversion of radio occultation signals. *Radio Sci.*, **38**, 1040, doi:10.1029/2002RS002763.

Kuo, Y.-H., T.-K. Wee, S. Sokolovskiy, C. Rocken, W. Schreiner, D. Hunt, and R. A. Anthes, 2004: Inversion and error estimation of GPS radio occultation data. *J. Meteorol. Soc. Japan*, **82**, 507–531.

References and suggested reading

Kursinski, E. R. and G. A. Hajj, 2001: A comparison of water vapor derived from GPS occultations and global weather analyses. *J. Geophys. Res.*, **106**, 1113–1138.

Kursinski, E. R., G. A. Hajj, S. S. Leroy, and B. Herman, 2000: The GPS radio occultation technique. *Terrestrial, Atmospheric and Oceanic Sciences*, **11**, 53–114.

Melbourne, W. G., et al., 1994: The application of spaceborne GPS to atmospheric limb sounding and global change monitoring. JPL-Publication 94-18, Jet Propulsion Laboratory, California Institute of Technology, Pasadena, California.

Schreiner, W. S., S. V. Sokolovskiy, C. Rocken, and D. C. Hunt, 1999: Analysis and validation of GPS/MET radio occultation data in the ionosphere. *Radio Sci.*, **34**, 949–966.

Sokolovskiy, S., 2003: Effect of superrefraction on inversions of radio occultation signals in the lower troposphere. *Radio Sci.*, **38**, 1058, doi:10.1029/2002RS002728.

Sokolovskiy, S. V., 2001: Modeling and inverting radio occultation signals in the moist troposphere. *Radio Sci.*, **36**, 441–458.

Syndergaard, S., 1998: Modeling the impact of the Earth's oblateness on the retrieval of temperature and pressure profiles from limb sounding. *J. Atmos. Solar-Terr. Phys.*, **60**, 171–180.

Vorob'ev, V. V. and T. G. Krasil'nikova, 1994: Estimation of the accuracy of the atmospheric refractive index recovery from Doppler shift measurements at frequencies used in the NAVSTAR system. *Physics of the Atmosphere and Ocean*, **29**, 602–609.